http://dx.doi.org/10.2106/JBJS.20.02036

The following content was supplied by the authors as supporting material and has not been copy-edited or verified by JBJS.

Supplemental Materials

Materials

BV-265: BV-265 expression constructs, cell line development, protein expression and purification are described in detail elsewhere[1]. BV-265 is a homodimeric recombinant chimeric protein consisting of N-terminal amino acid sequences from human BMP-2, central amino acid sequences from human BMP-6, and C-terminal amino acid sequences from activin A (Fig. S1). The particular amino sequences were specifically engineered to optimize BMP receptor-binding and minimize inhibition by soluble BMP antagonists, such as noggin and Gremlin, based on the crystal structure of BMP/receptor and BMP/antagonist complexes. These sequences also maintain the disulfide-linked dimer structure and three intra-chain disulfide bonds, forming the disulfide-knot structure characteristic of transforming growth factor-beta (TGF-β) superfamily of proteins and present minimally altered native BMP surface amino acid sequences to reduce potential antigenicity. BV-265 is produced in Chinese Hamster Ovary cell line genetically engineered to contain the vectored cDNA constructs. Like all TGF-β proteins, BV-265 is synthesized as a large precursor molecule proteolytically cleaved within the cell to yield a mature glycosylated BV-265 homodimer with each subunit containing the carboxyterminal portion of the peptide chain. Purification includes three column chromatography steps, a viral clearance filtration step and a tangential flow ultrafiltration step to exchange the protein into formulation buffer and to concentrate the active protein after the final filtration. The resulting liquid BV-265/formulation buffer drug substance is aseptically filtered then frozen for storage.

BMP-2: BMP-2, produced in a similar manner as BV-265, was supplied by Pfizer Inc (Andover MA).

Composite Matrix (manufactured at LSNE Bedford NH): The composite matrix (CM) is composed of high specific-surface area calcium-deficient hydroxyapatite granules (CDHA) containing both macropores and micropores suspended in a macroporous, fenestrated, polymer mesh-reinforced recombinant human type I collagen (rhCollagen) matrix (**Fig. 1-A and 1-B**). Composition, manufacturing and characterization of the CM is described in detail elsewhere[1]. Briefly, the CM was manufactured by combining the CDHA granules with a 1-ethyl-3-(3-dimethylaminopropyl)carbodiimide (EDC) cross-linked rhCollagen solution to yield a slurry. The slurry and polymer mesh were placed in a mold containing an array of 1.5 mm pins. The composite slurry was lyophilized, cross-linked with EDC a second time and rinsed with purified water. The CM was then coated with a thin layer of rhCollagen and lyophilized a second time. The CM was packaged using a PETG blister pack with a Tyvek seal and the sealed tray was then placed in a secondary Tyvek pouch. The CM was terminally sterilized with ethylene oxide.

The CM was engineered for optimal BV-265 retention and guided tissue repair. Macroporosity was supplied by a combination of the intrinsic porosity of the rhCollagen matrix and fenestrations. The polymer mesh was embedded within the rhCollagen matrix to increase matrix stiffness and shear resistance during handling and surgical placement. The top and bottom surfaces of the CM were coated with a 0.5 mm layer of rhCollagen to minimize CDHA granule shedding during handling and surgical placement.

CDHA Granules (Mathys LTD Bettlach, Switzerland): A slurry of calcium sulfate ($CaSO_4$) powder, starch, cellulose and water was thoroughly mixed and dried into uniform blocks. The starch and cellulose were used both as binders and to induce porosity within the material. The blocks were crushed and sintered at 750°C to induce a phase transformation to anhydrous $CaSO_4$ and remove the binding/pore forming materials. This material was then milled and sieved. A final phase transformation to CDHA was induced via incubation in a liquid solution of ammonium phosphate. The CDHA granules were thoroughly washed in deionized water, dried and sieved to obtain granules of the desired size range from 0.4 to 0.8 mm.

Type I rhCollagen (Collplant Rehovot, Israel): Type I rhCollagen was produced using an expression system in tobacco plants. Parent tobacco plants expressing 5 human genes for Type I human collagen (COL1a1 and COL1a2) and enzymes for assembling and processing the collagen precursor molecules (P4Ha, P4Hb, LH-3) were generated through successive transfections and crossing. As the tobacco matures, human Procollagen is produced and stored in the vacuole system of the plants. Through a combination of mechanical and biochemical processes the human Procollagen is extracted and purified from the plants. The Procollagen is then enzymatically processed and purified into the final raw material[2].

PGLA Polymer Mesh (Confluent Warwick, RI): The polymer mesh was made from a Poly(glycolide-*co*-lactide) co-polymer (PGLA) blend using a knitting process resulting in a 0.2-0.3 mm thick mesh with > 1.0 mm openings.

Porous Composite Matrix (manufactured at LSNE Bedford NH): The porous composite matrix (PCM) was manufactured by combining CDHA granules with a bovine collagen solution to yield a slurry. The slurry was placed in a mold containing an array of 1.5 mm pins and lyophilized to form the PCM. The lyophilized PCM was cross-linked with glutaraldehyde aqueous solution and washed in purified water. Finally, the PCM was lyophilized again and terminally sterilized by gamma irradiation. Macroporosity was supplied by a combination of the intrinsic porosity of the bovine collagen matrix and fenestrations.
Bovine collagen (Devro Pty Limited, Bathrust, Australia): The bovine collagen matrix was derived from bovine hide.

Absorbable Collagen Sponge: The bovine type 1 absorbable collage sponge was supplied by Pfizer Inc (Andover MA).

MASTERGRAFT® *Matrix rods*: The HA/TCP/bovine collagen MASTERGRAFT® Matrix rods (MM) were from Medtronic. (Memphis TN).

Methods

Rodent ^{125}I-labeled BV-265/CM, BV-265/PCM, BMP-2/ACS, and BMP-2/buffer retention

Study design: Retention of ^{125}I-labeled-BV-265 and BMP-2 in the designated carriers was determined using in vivo scintigraphy following implantation or injection in a rodent muscle pouch over a 10-week

period or until values reached background (Table 1). Area under the percent retention versus time curves (AUC) for 0-1, 0-2, or 0-10 weeks was determined for each treatment group depending on the duration of the individual group retention profiles. Retention profiles were determined from 6 animals per treatment group.

Study animals: A total of 24 female Long Evans rats (approximately 8 to 8.5 weeks of age, 183 to 222 g) were obtained from Charles River Laboratories. During the 7 to 10-day acclimation period, the animals were observed daily with respect to general health and any signs of disease. All animals were given a detailed clinical examination prior to selection for study. The animals were housed in individual solid bottom cages with nonaromatic bedding in an environmentally controlled, light cycled room. Animal enrichment was provided. Standard certified solid rat chow was available ad libitum and tap water was available ad libitum via an automatic watering system.

Implant preparation: A solution of ^{125}I-labeled-BV-265 and unlabeled BV-265 or ^{125}I-labeled-BMP-2 and unlabeled BMP-2 was prepared with 25 μCi/implant activity. In all cases the ^{125}I-labeled-cytokine was < 5% of total cytokine dose. ^{125}I-labeled-cytokine was prepared by PerkinElmer using a modified Iodogen (R) procedure. Labeled cytokine was purified by open column chromatography. This method predominantly labels tyrosine residues. Radiochemical purity was initially found to contain < 5% free iodide at time of preparation by instant thin-layer chromatography (iTLC). Radiochemical purity of ^{125}I-labeled-cytokine added to the unlabeled cytokine solution was confirmed to be < 5% free iodide by iTLC on the day of surgery.

The ^{125}I-labeled-BV-265/CM and PCM implants were formulated from a 6.0 mm x 4.0 mm diameter segment of CM or PCM (113 μL) loaded with 43 μL (38% soak-load) of 0.261 μg/μL ^{125}I-labeled-BV-265 + unlabeled BV-265 solution to yield a final concentration of 0.1 mg/cm^3 BV-265/CM or PCM and a total dose of 11.3 μg.

The ^{125}I-labeled-BMP-2/ACS implants were formulated with three 6.0 mm x 3.0 mm segments of ACS (255 μL total volume) sutured together to form a single implant, loaded with 67.5 μL (30% soak-load) of 0.37 μg/μL ^{125}I-labeled-BMP-2 + unlabeled BMP-2 solution to yield a total dose of 25 μg. The ^{125}I-labeled-BMP-2/buffer injections were formulated by injecting 100 μL of 0.4 μg/μL ^{125}I-labeled-BMP-2 + unlabeled BMP-2 solution into the biceps femoris to yield a 40 μg total dose.

Surgery/Injection: The hind limbs of adult Long Evans rats were shaved and disinfected with 70% isopropanol and betadine solution under general anesthesia induced and maintained on isoflurane inhalation anesthesia. A fenestrated sterile paper drape was placed to allow access to both hind limbs. With the animal in lateral recumbency, a stab incision in the skin overlying the middle of the biceps femoris was continued through the subcutaneous tissue and fascia. The middle of the muscle belly was accessed with blunt dissection and the closed tip of a small Mayo scissors was inserted into the muscle and then spread apart to create a pocket. The designated test article was then placed into the muscle pouch. The overlying soft tissues and skin were closed with absorbable suture and the skin incision was sealed with surgical adhesive. The BMP-2/formulation buffer injection were performed with a 0.5-mL syringe equipped with a 21-gauge needle. Animals were euthanized by CO_2 inhalation at the termination of the study. Animal carcasses were stored frozen until they returned to background radiation levels and were then incinerated.

Retention profiles: Scintigraphic imaging of the ^{125}I-labeled-BV-265 implants and ^{125}I-labeled-BMP-2 implants/injections were performed on a nanoScan SPECT/CT (Mediso Medical Imaging Systems). Image acquisition and reconstruction were performed using Mediso Nucline V2.0 software. Image analysis was performed using VivoQuant V2.5 software (Invicro, LLC). Scintigraphic images were acquired immediately after implantation, on days 1, 3, 5, 7 and 10 and then weekly for a total of 10 weeks or whenever radiation returned to background with the animals induced and maintained on isoflurane inhalation anesthesia. At each time point, a planar gamma camera image of each animal with ^{125}I-labeled implant or injection was obtained (Energy window: 24.14 - 32.66 keV; Collimator zoom = 1.14). The animals were always placed in the same position on the gamma camera head with the limbs in the same orientation to minimize variability. The acquisition length was sequentially increased from a 5-minute scan on day zero to compensate for radioactive decay and clearance of the labeled cytokine from the implantation or injection site over the course of the study. Standard sources were placed within the field of view of each scan to ensure that camera performance was consistent throughout the course of the study. Retention data were corrected for ^{125}I radioactive decay. Retention profiles were determined from 6 animals per treatment group and were expressed as a percentage of the initial measurement. Area under the percent retention versus time curves (AUC, fraction*days) was determined using the trapezoid method for 0-1, 0-2 and or 0-10 weeks for each treatment group depending on the duration of the individual group retention studies.

Non-human primate non-instrumented posterolateral fusion (PLF)

Study design: Efficacy of the CM, BV-265/CM, BV-265/PCM and BMP-2/ACS:MM combinations was evaluated in a series of studies utilizing a non-instrumented PLF model in adult male rhesus macaques (Table 1). The non-instrumented PLF model was selected to provide a more challenging fusion environment compared to additional of posterior stabilization. The well tolerated non-instrumented PLF model also required less post-operative manipulation of the animals compared to pilot studies using PLF with posterior stabilization. The use of posterior stabilization resulted in incisional complications requiring additional post-operative anesthesia procedures for treatment and prevention.

The first exploratory study utilized left and right L3/4 and left and right L5/L6 hemivertebral motion segment PLFs in 1 animal each euthanized at 4 or 12 weeks. This study compared CM alone to 0.05, 0.15 or 0.25 mg/cm^3 BV-265/CM (total dose = 12, 42 or 70 mg per side, respectively) in 1 each of the 4 available hemivertebral motion segment PLFs per animal.

The second study utilized L3/L4 or L5/L6 motion segment PLFs distributed in 9 animals euthanized at 24 weeks. This study expanded evaluations of CM (0.0 mg BV-265 per side, n = 3 motion segments) and 0.05 mg/cm^3(0.12 or 0.14 mg BV-265 per side, 0.24 or 0.28 mg BV-265 total dose, n = 4 motion segments) BV-265/CM and focused on the 0.15 mg/cm^3 (0.36 or 0.42 mg BV-265 per side, 0.72 or 0.84 mg BV-265 total dose, n = 11 motion segments) BV-265/CM combination as the potential lead BV-265 concentration/dose. The 0.25 mg/cm^3 BV-265/CM (0.7 mg BV-265 per side) combination was not evaluated in this study based on the excessive volume of the fusion mass observed in the first study. Although useful to limit the number of animals required in this initial concentration/dose ranging study,

the presence of an untreated motion segment between two treated motion segments introduces the potential for adverse mechanical forces complicating successful fusion.

The third study utilized a two-level L3/L4/L5 motion segment PLF in 15 animals. The two level PLF model was selected to mimic more challenging multi-level fusions performed in human clinical cases. This study evaluated a 0.25 mg/cm^3 BV-265/CM combination (0.6 mg BV-265 per side, 1.2 mg total BV-265 dose) utilizing a thinner CM (4.0 mm) compared to the first study (8.0 mm) in 1 animal each euthanized at 12 weeks and 2 animals each euthanized at 24 weeks. The thinner CM was selected to limit the volume of the fusion mass observed to be excessive in response to the thicker CM used in the first study. The third study also compared 0.075, 0.15 or 0.3 mg/cm^3 BV-265/PCM (0.43, 0.86 or 1.73 mg BV-265 per side, respectively; and 0.86, 1.72 and 3.46 mg total BV-265 dose, respectively) in 1 animal each euthanized at 12 weeks and 2 animals each euthanized at 24 weeks. The PCM was introduced as a bovine collagen alternative to the rhCollagen CM with a less complex structure and associated manufacturing process. The BV-265/CM and PCM fusions were compared to 0.43 mg/cm^3 BMP-2/ACS:MM (1.72 mg BMP-2 per side, 3.43 mg total BMP-2 dose) in 1 animal each euthanized at 12 weeks and 2 animals each euthanized at 24 weeks. The BMP-2 concentration was selected to deliver a BMP-2 dose per side and total BMP-2 dose equivalent to the 0.3 mg/cm^3 BV-265/PCM group. The combination BMP-2 soak-loaded ACS wrapped around dry MM mimics BMP-2/carrier combinations frequently used in clinical practice.

Outcome assessments: In vivo computed tomography (CT) images of the nonhuman primate PLFs were obtained after surgery and at 4, 8, 12 and 24 weeks, where applicable **(Figs. S2 and S3)**. Manual palpation, explant micro or nano computed tomography (μCT or nCT) and histological evaluations were performed following euthanasia. Fusion, assessed in a blinded manner by two of the authors, required evidence of solid fusion on explant manual palpation, continuous radiographic and histological evidence of bone integrating into and spanning adjacent transverse processes.

Study animals: The male rhesus monkeys (*Macaca mulatta*) used for this study had mean body weight and standard deviation of 12 ± 2 kg and were between 5 to 10 years old. They were obtained from a disease free captive-bred colony (The Mannheimer Foundation Inc, Homestead FL). The animals were acclimated in an Association for Assessment and Accreditation of Laboratory Animal Care accredited, limited access facility for a minimum of 2 weeks prior to initiating the study. The animals were housed in single large cages. They were fed Monkey Chow from an approved supplier supplemented with fruits and had access to water ad libitum. The animals participated in an enrichment program prescribed by the institutional animal care staff. All of the animals were weighed and had routine physical examinations performed by the institutional lab animal veterinarian prior to the start of the study. Laboratory screening tests performed prior to enrollment in the study included a baseline CBC, serum chemistry profile, tuberculosis test, and virus titer screens (herpes B-virus, Measles, Simian Retrovirus, Simian Immunodeficiency Virus, Simian T-cell Leukemia Virus). Only animals determined to be suitable by the institutional veterinarian were enrolled in the study. The general health and well-being of the animals was

monitored throughout the study. Prior to surgery, the physical examination was repeated and any pre-surgical laboratory tests deemed to be required by the LAR veterinarian were performed.

Implant preparation: The CM and BV-265/CM implants for the 4/12-week BV-265 concentration/dose ranging study were formulated with 30 mm long/10 mm wide/8 mm thick or 35 mm long/10 mm wide/8 mm thick segments of the CM for the L3/L4 and L5/L6 motion segments, respectively (Table 1). The former were soak-loaded with 0.92 mL of 0.0 or 0.13 mg/mL BV-265/buffer solution to yield a 0.0 mg/cm^3 (CM control) or 0.05 mg/cm^3 BV-265/CM concentration, respectively, and a 0.0 mg (CM control) or 0.12 mg total BV-265 dose, respectively. The latter were soak-loaded with 1.07 mL of 0.39 and 0.65 mg/mL BV-265/buffer solution to yield a 0.15mg/cm^3 or 0.25 mg/cm^3 BV-265/CM concentration, respectively, and a 0.42 or 0.7 mg total BV-265 dose, respectively.

The BV-265/CM implants for the 24-week BV-265 concentration/dose ranging study were formulated with 30 mm long/10 mm wide/8 mm thick or 35 mm long/10 mm wide/8 mm thick segments of the CM for the L3/L4 and L5/L6 motion segments, respectively (Table 1). The former were soak-loaded with 0.92 mL of 0.0, 0.13 or 0.39 mg/mL BV-265/buffer solution to yield a 0.0 mg/cm^3 (CM control), 0.05 or 0.15 mg/cm^3 BV-265/CM concentration, respectively; a 0.0 mg (CM control), 0.12 or 0.36 mg BV-265 dose per side, respectively; and a 0.24 or 0.72 BV-265 total dose, respectively. The latter were soak-loaded with 1.07 mL of 0.13 or 0.39 mg/mL BV-265/buffer solution to yield a 0.05mg/cm^3 or 0.15 mg/cm^3 BV-265/CM concentration, respectively; a 0.14 or 0.42 mg BV-265 dose per side, respectively; and a 0.28 or 0.84 mg BV-265 total dose, respectively.

The BV-265/CM implants for the 12/24-week L3/L4/L5 BV-265/CM study were formulated with 30 mm long/10 mm wide/4 mm thick segments of the CM for both the L3/L4 and L4/L5 motion-segments (Table 1). The CM segments were soak-loaded with 0.42 mL of 0.72 mg/mL BV-265/buffer solution to yield a 0.25 mg/cm^3 BV-265/CM concentration, a 0.3 mg BV-265 dose per implant, a 0.6 mg BV-265 dose per side, and a 1.2 mg BV-265 total dose. The BV-265/PCM implants were formulated with 30 mm long/12 mm wide/8 mm thick segments of the PCM for both the L3/L4 and L4/L5 motion-segments. The PCM segments were soak-loaded with 0.864 mL of 0.25, 0.5 or 1.0 mg/mL BV-265/buffer solution to yield a 0.075, 0.15 or 0.3 mg/cm^3 BV-265/PCM concentration, respectively; a 0.22, 0.43 or 0.87 mg BV-265 dose per implant, respectively; a 0.43, 0.86 or 1.73 mg BV-265 dose per side, respectively; and a 0.86, 1.72 and 3.46 mg BV-265 total dose, respectively.

The BMP-2/ACS:MM implants were formulated with 51 mm long/38 mm wide/1 mm thick segments of BMP-2/ACS wrapped around a 30 mm long/10 mm wide/10 mm thick MM rod. The ACS segments were soak-loaded with 2.0 ml of 0.43 mg/mL BMP-2/buffer solution to yield a 0.43 mg/cm^3 BMP-2ACS concentration, a 0.86 mg BMP-2 dose per implant, a 1.72 mg BV-265 dose per side, and a 3.42 mg total BV-265 dose. The applied BMP-2 solution was allowed to equilibrate with the ACS for 15 minutes prior to wrapping around the dry MM rod.

Surgery: The animals were food-fasted 12 hours and administered intra-muscular Naxcel (Ceftiofur, 2.2 mg/kg) and Glycopyrrolate (0.004-0.008 mg/kg). Following sedation with Telazol (tiletamine and zolazepam, 3 to 5 mg/kg intramuscularly), the animals were intubated and general anesthesia was maintained with isoflurane/O_2. A 0.9% sodium chloride solution was administered during surgery through

an intravenous catheter placed in the brachial vein. The animals were positioned in sternal recumbency and manual palpation of the iliac crests in conjunction with preoperative lateral to medial and dorsal to ventral plain film radiographs was used to estimate the location of L3/4, L4/5 and L5/6. Prior to final aseptic preparation of the surgical site, approximately 1 ml of 0.5% Lidocaine was injected subcutaneously along the length of the proposed surgical incision. Animals were monitored during anesthesia using standard evaluation techniques including ECG and pulse oximetry. Sterile preparation and draping was then performed with the animals in sternal recumbency. A midline incision was used to expose the lumbodorsal fascia. The fascia and the paraspinal muscles were carefully stripped subperiosteally with a Cobb elevator and electrocautery from the spinous processes and laminae to the transverse processes. The transverse processes of L3/L4 or L5/L6 vertebra for single level fusions or L3/L4/L5 vertebra for two level fusion, and the intertransverse membrane were then exposed, leaving the facet joints intact. The dorsal aspects of the exposed transverse were decorticated using a high-speed burr until bleeding surfaces with cancellous bone were observed. The designated implant was then placed over the decorticated transverse processes and associated paraspinal muscle bed between adjacent transverse processes on each side of the spine at the designated levels. The overlying fascia was closed with closed with 3-0 absorbable suture in a continuous interlocking pattern. The skin incision was closed with 3-0 absorbable sutures placed in a subcuticular pattern. Skin staples or surgical glue was used at the surgeon's discretion to augment skin closure to limit the potential for postoperative incisional dehiscence.

Post-surgery care: Animals were administered subcutaneous Buprenorphine SR analgesic (0.2 mg/kg) once after surgery and subcutaneous Meloxicam (0.1-0.2 mg/kg) once per day for seven days. Antibiotic treatment was continued once per day for 7 days after the surgery. Animals were monitored daily for appetite, attitude, activity level, fecal/urine output, wound healing and behavioral changes (i.e. licking, biting, scratching, teeth grinding, depression). Body weights were obtained every other week for 2 weeks then monthly. Buprenorphine and/or Flunixin meglumine at 0.5 to 1.0 mg/kg IM was administered on an "as needed" basis for extended analgesia or anti-inflammatory action. Staples were removed 14 days after surgery depending on the assessment of the surgical site healing.

In vivo computed tomography (CT): In vivo CT images were obtained after surgery and at the designated times with a combination of intramuscular Glycopyrrolate (0.004-0.008 mg/kg) and Ketamine (10-30 mg/kg). The CT images were obtained with a CereTom portable spiral CT scanner (Universal Medical Systems, Solon, OH) set to 120 kVp, 6 mA, 12,000 μAs exposure, 0.368 mm isotropic voxel size and 170 mm scan length.

Harvest of the spinal segments: Animals were euthanized by barbiturate overdose at the end of the study. The previous surgery site was then opened and the soft tissue attachments to the designated spinal segments were released by a combination of blunt and sharp dissection. The designated spinal segments were then removed with an oscillating saw. The spinal segments were labeled, wrapped with sterile gauze sponges and placed in specimen bags containing formalin for storage prior to μCT or nCT imaging and histological processing.

Manual Palpation: Following harvest the spinal segments were manipulated in a blinded fashion by two of the authors for dorsal-ventral, lateral-medial and rotational stability. Verification of fusion required stability in all three directions.

μCT imaging: The L3/L4 and L5/L6 spinal segments were sectioned in the sagittal plane and then trimmed with a band saw to generate left and right hemivertebrae motion segment spinal sections of appropriate size for imaging. The L3/L4/L5 spinal segments evaluated with μCT were first divided in the axial plane through the L4 vertebral body and then prepped in the sagittal plane in a similar manner as described for the single level spinal segments to generate left and right hemivertebral motion segment specimens of suitable size for imaging. The specimens were then imaged with a high-resolution μCT (Scanco μCT40; Scanco Medical AG) with 70 kVp source voltage, 57 μA source current, 30.0 μm pixel size, 250 projections over a 360° rotation, and a 0.2 seconds integration time. On average, 1800 slides per sample were reconstructed using the included Scanco software. A global fixed threshold value (7208 native grey levels, 220 mg HA/cm^3) was applied to all data. The 3-D reconstructed images and the associated axial, sagittal and coronal slice-images were evaluated in a blinded manner by three of the authors. Verification of fusion, assessed in a blinded fashion by two of the authors, required bone integration into the transverse processes and continuous bone spanning the region between adjacent transverse processed.

nCT imaging: The BV-265/PCM and BMP-2/ACS:MM specimens were imaged with nCT (Xradia 520 Versa, Carl Zeiss Microscopy, Jena, Germany) with a 25W X-ray source. Images were obtained from intact bilateral L3/L4/L5 specimen without the need for further dissection described above for μCT imaging. The spinal segments were immersed in 70% ethanol and scanned at spatial resolution of 500 nm with a minimum achievable voxel size of 40 nm. Approximately 1,500 to 1,800 slides per sample were reconstructed. Images were reconstructed using XMReconstructor (Zeiss) and evaluated using ImageJ. The 3-D reconstructed images and the associated axial, sagittal and coronal slice-images were evaluated in a blinded manner by three of the authors. Verification of fusion , assessed in a blinded fashion by two of the authors, required bone integration into the transverse processes and continuous bone spanning the region between adjacent transverse processed.

Histological specimen preparation: A Low Speed Isomet (Buehler, Lake Bluff, IL) was used to cut the spinal segments to the appropriate size for imbedding. The sectioned vertebral specimen blocks was marked with permanent ink for orientation purposes. Each specimen block was placed into labeled processing bags and immersed into fresh 70% ethanol for fixation.

The specimen blocks were processed through alcohol gradients (cleared in xylene) under vacuum and gentle agitation in the Fisher LX 120 Automatic Tissue Processor. Specimen blocks were infiltrated and embedded in methyl methacrylate and allowed to polymerize for 3 to 5 days at room temperature following previously published methods with slight modifications[3]. After polymerization was complete, the specimen blocks were removed from their molds and prepared for thin-sectioning. Specimens were sectioned to 5.0 thickness using a Riechert/Leica Jung Polycut (Leica Biosystems, Buffalo Grove, IL). Sections from each specimen block were stretched and pressed on gelatin chrome-alum slides and placed in an oven at 45°-50° C overnight (minimum) to ensure tissue adherence to the slides. Slides were then allowed to reach room temperature prior to staining. The 5.0 μm sections were stained with Goldner's trichrome. Histological specimens were evaluated in a blinded manner with light microscopy by 2 of the authors. Verification of fusion, assessed in a blinded fashion by 2 of the authors, required histological evidence of bone integration into the transverse processes and continuous bone spanning the region between adjacent transverse processed.

Supplemental References

1. Seeherman HJ, Berasi SP, Brown CT, Martinez RX, Juo ZS, Jelinsky S, Cain MJ, Grode J, Tumelty KE, Bohner M, Grinberg O, Orr N, Shoseyov O, Eyckmans J, Chen C, Morales PR, Wilson CG, Vanderploeg EJ, Wozney JM. A BMP/activin A chimera is superior to native BMPs and induces bone repair in nonhuman primates when delivered in a composite matrix. Sci Transl Med. 2019;11(489):eaar4953.

2. Stein H, Wilensky M, Tsafrir Y, Rosenthal M, Amir R, Avraham T, Ofir K, Dgany O, Yayon A, Shoseyov O. Production of bioactive, post-translationally modified, heterotrimeric, human recombinant type-I collagen in transgenic tobacco. Biomacromolecules. 2009;10(9):2640-5.

3. Schenk RK, Olah AJ, Herrmann W. Preparation of calcified tissues for light microscopy. In Dickson GR, editor. Methods of Calcified Tissue Preparation. Amsterdam: Elsevier; 1984. p 1-56.

Supplemental Figures

http://dx.doi.org/10.2106/JBJS.20.02036

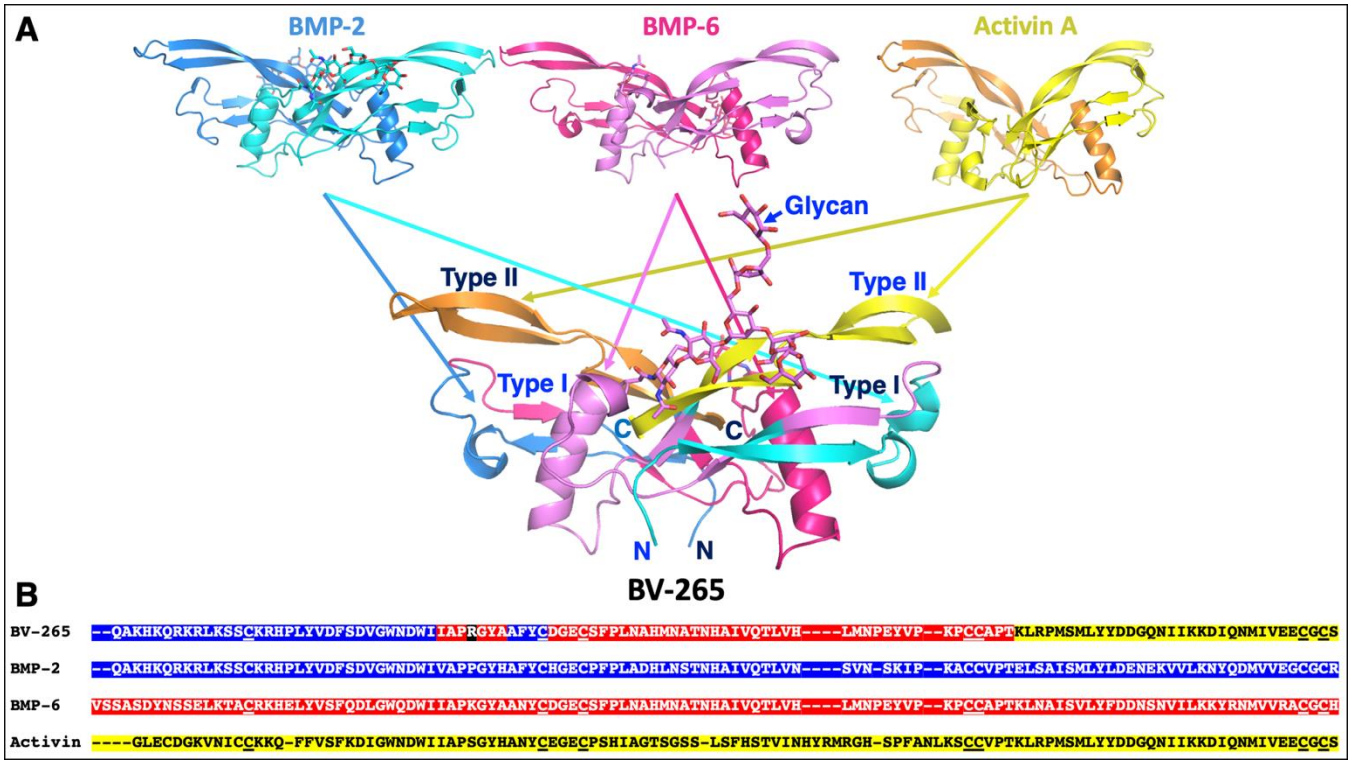

Fig. S1

Figs. S1-A through S1-B Ribbon structures and corresponding amino acid sequence alignment of BMP-2, BMP-6, activin A and BV-265[1]. **Fig. S1-A** Ribbon diagrams of glycosylated BMP-2 (cyan/blue), glycosylated BMP-6 (pink/magenta), activin A (yellow/orange), and glycosylated BV-265 (multi-colored) in the "butterfly" orthogonal view. Sections of the chimera ribbon diagrams representing amino acid sequences originating from the BMP-2, BMP-6 and activin A are depicted in the color of the corresponding parental molecule. Labels indicating the location of the type I and II BMP receptor binding domains for each monomer are located next to or superimposed on the BV-265 ribbon diagram (monomer 1 = dark blue, monomer 2 = blue). Only one BV-265 monomer displayed a resolved glycan in the crystal structure. The glycan of the second monomer was disordered due to crystal packing artifact. **S1-B** Amino acid sequence alignment for BMP-2 (blue), BMP-6 (magenta), activin A (yellow) and BV-265 monomers (multi-color). Amino acid sequences substituted into the chimeras are represented by the corresponding colors of the parental molecules.

http://dx.doi.org/10.2106/JBJS.20.02036

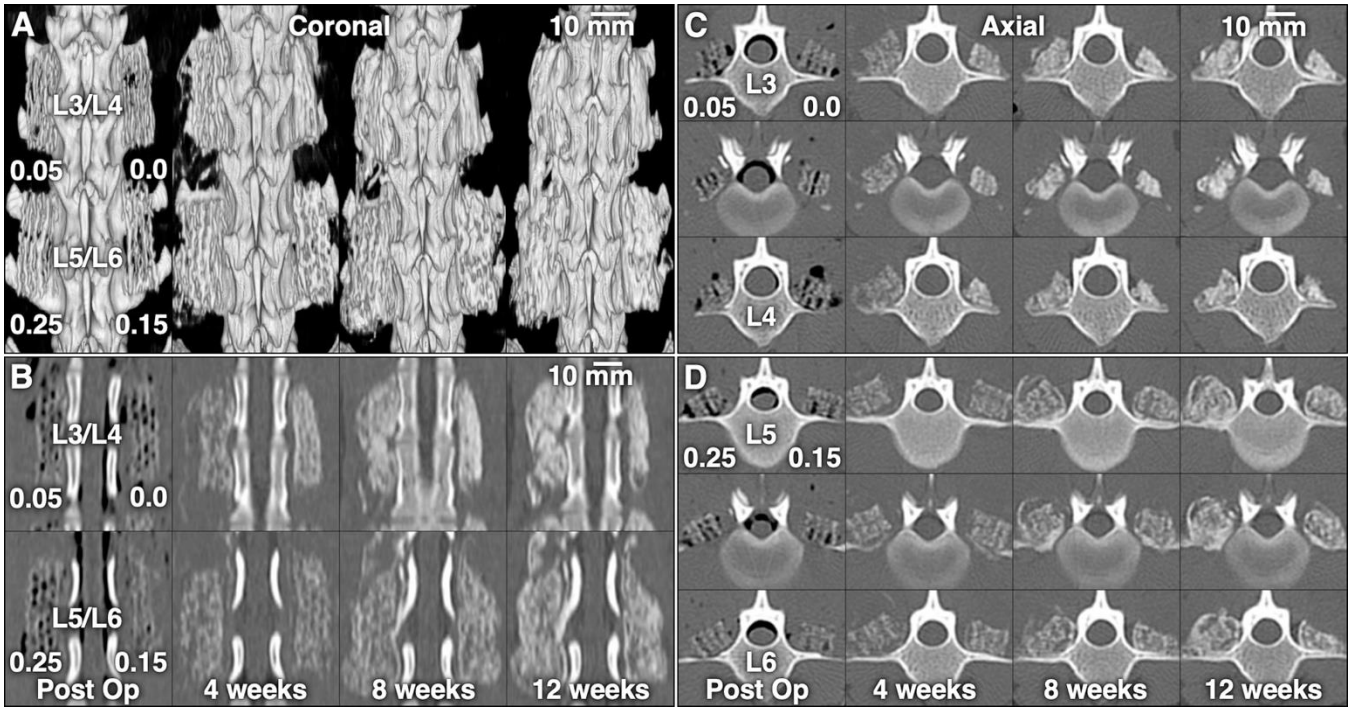

Fig. S2

Figs. S2-A through S2-D In vivo CT time-series images of the CM and BV-265/CM-treated nonhuman primate hemivertebral motion segments over the 12-week study duration. **Fig. S2-A** In vivo coronal 3D CT reconstructions of the nonhuman primate with L3/L4 hemivertebrae motion segment treated with CM alone (0.0) or 0.05 mg/cm^3 BV-265/CM (0.05) and L5/L6 hemivertebrae motion segment treated with 0.15 mg/cm^3 (0.15) or 0.25 mg/cm^3 (0.25) BV-265/CM immediately after surgery (Post-op) and at 4, 8 and 12 weeks. **Fig. S2-B** Corresponding coronal CT time-series slice images. **Figs. S2-C and S2-D** Corresponding axial CT time-series images. Radiodense regions consistent with bone formation adjacent to and between the decorticated transverse processes are present in all the BV-265/CM-treated motion segments.

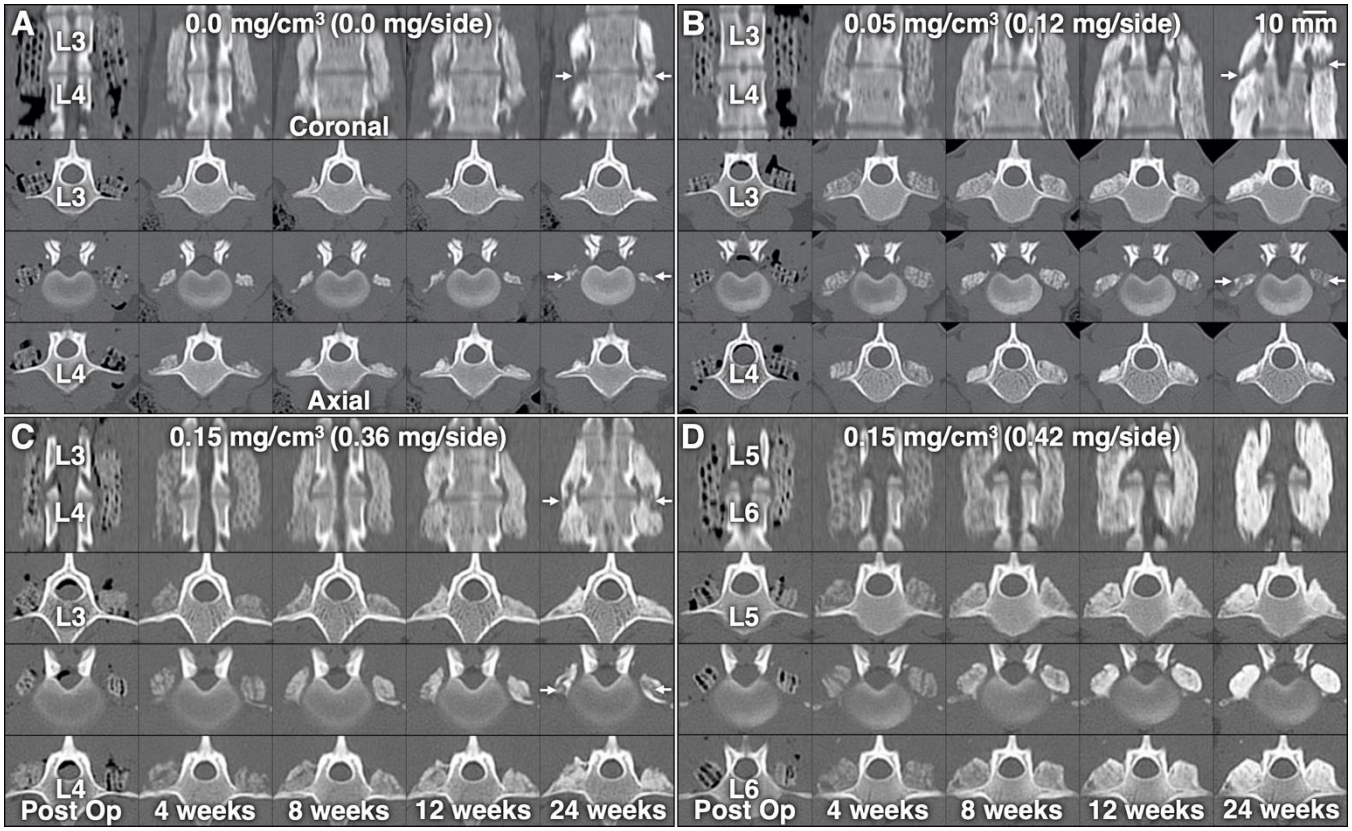

Fig. S3

Figs. S3-A through S3-D In vivo CT time-series images of the CM and BV-265/CM-treated nonhuman primate L3/L4 or L5/6 hemivertebral motion segments over the 24-week study duration. In vivo CT time-series images of the CM and BV-265/CM-treated nonhuman primate L3/L4 or L5/6 motion segment PLF over a 24-week study duration. **Fig. S3-A through S3-D** In vivo coronal and axial CT slice images of representative nonhuman primates with an L3/L4 motion segment implanted with CM (0.0 mg/cm^3), an L3/L4 motion segment implanted with 0.05 mg/cm^3 BV-265/CM, and an L3/L4 motion segment implanted with 0.15 mg/cm^3 BV-265/CM, and an L5/L6 motion segment implanted with 0.15 mg/cm^3 BV-265/CM immediately after surgery (Post-op) and at 4, 8, 12 and 24 weeks. Radiodense regions consistent with bone formation adjacent to the decorticated transverse processes are present in all the motion segments. Bilateral radiolucent regions (white arrows) between adjacent transverse processes consistent with the lack of bone formation are present in the representative CM **(Fig. S3-A)**, 0.05 mg/cm^3 BV-265/CM **(Fig. S3-B)** and one of the 0.15 mg/cm^3 BV-265/CM (**Fig. S3-C**). Continuous bilateral radiodense regions consistent with bone bridging between adjacent transverse processes is present in the second 0.15 mg/cm^3 BV-265/CM (**Fig. S3-D**).